

# Hyperon photo- and electroproduction at CLAS

S.P. Barrow<sup>a</sup>, representing the CLAS collaboration

<sup>a</sup>Florida State University  
Tallahassee, Florida, 32306

(Received: November 21, 2018)

The large acceptance and high multiplicity capabilities of the CLAS detector make it possible to study a wide range of previously unmeasured strange baryon production processes. Studies of the decay angular distributions of electroproduced strange baryons have yielded several interesting new results. The  $\Lambda(1520)$  electroproduction decay angular distributions shed light on the spin projections of the  $\Lambda(1520)$ . Analysis of the decay angular distributions of the weakly decaying  $\Lambda(1116)$  have revealed the induced baryon polarization due to unpolarized incident electron beams. In addition to these topics, other features of the CLAS strange baryon program, such as photoproduction and virtual photon L-T decompositions, are also briefly summarized.

## 1 Introduction

The hyperon physics program at CLAS uses polarized and unpolarized electron beams, with incident energies ranging from 2.4 to 6.0 GeV, to study hyperon photo- and electroproduction. A complete list of all approved analysis projects currently underway is summarized in Table 1. These experiments measure such aspects of hyperon production as the production cross sections and the corresponding response functions, the hyperon decay angular distributions, and the radiative decay strengths of the light hyperons.

Experiment	Title	Spokesperson(s)
E89-004	Hyperon photoproduction	R. Schumacher
E89-024	Radiative decays of light hyperons	G. Mutchler
E89-043	$\Lambda(1116)$ , $\Lambda(1520)$ and $f_0(980)$ electroproduction	L. Dennis, H. Funsten
E93-030	Structure functions for kaon electroproduction	K. Hicks, M. Mestayer
E95-003	$K^0$ electroproduction	R. Schumacher, K. Dhuga
E99-006	Polarization observables in $p(\vec{e}, e'K^+)\Lambda$	D. Carman, K. Joo, L. Kramer, B. Raue
CAA-2000-1	$K^*$ electroproduction	K. Hicks

Table 1. The strange baryon production experiments at CLAS.

The large acceptance of the CLAS detector makes it possible to study hyperon production over a wide kinematic regime. In addition, its high multiplicity capabilities enable the study of sequential processes such as decay angular distributions of electroproduced hyperons. Due to time constraints, the remainder of this talk will focus on the results of measurements of  $\Lambda(1520)$  decay angular distributions (E89-043), as well as  $\Lambda(1116)$  decay using unpolarized (E89-043) electron beams. The kinematic regimes presented here have not been studied in any previous measurements.

## 2 $\Lambda(1520)$ decay angular distributions

The CLAS event reconstruction is based on the missing mass technique to identify the mass of neutral hyperons and undetected particles. A study of electroproduction decay angular distributions requires detecting the scattered electron and at least two hadrons, and the  $\Lambda(1520) \rightarrow p - K^-$  decay mode of the  $\Lambda(1520)$  is the one best suited for study with CLAS. Figure 1 shows the relevant

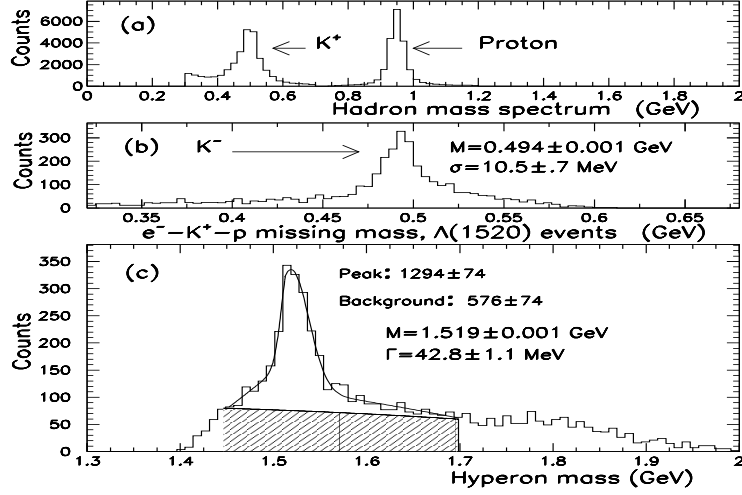


Figure 1: (a) The hadron mass spectrum for events that contain a proton track and a  $K^+$  candidate. (b) The  $K^-$  missing mass spectrum for events in which the  $e^-K^+$  missing mass is consistent with the  $\Lambda(1520)$  mass. (c) The hyperon mass spectrum for the  $e^-K^+K^-p$  final state. A cut on the  $K^-$  missing mass from 0.455 to 0.530 GeV was used to generate this hyperon spectrum.

missing mass plots for  $\Lambda(1520)$  electroproduction data taken as part of the 1998 and 1999 E1 run periods with beam energies of 4.05, 4.25, and 4.45 GeV. Reactions that produce other hyperons, such as the  $\Lambda(1405)$ ,  $\Sigma(1480)$ , and  $\Lambda(1600)$ , account for the majority of the background under the  $\Lambda(1520)$  peak, but the relative contributions from the individual processes are currently unknown. A complete listing of the hyperons whose mass and width have some overlap with the  $\Lambda(1520)$  peak is presented in Ref. [1].

A measurement done at Daresbury of  $\Lambda(1520)$  photoproduction [2] used incident photons with energies ranging from 2.8 to 4.8 GeV (total center-of-mass energy  $W$  from 2.5 to 3.1 GeV), and reports an exponential  $t$ -dependence dominated by  $t$ -channel exchange of the  $K^*(892)$  meson, and not the lighter  $K(494)$  meson. A thorough understanding of the reasons  $\Lambda(1520)$  photoproduction proceeds mainly through the exchange of a heavier vector meson requires theoretical studies of the

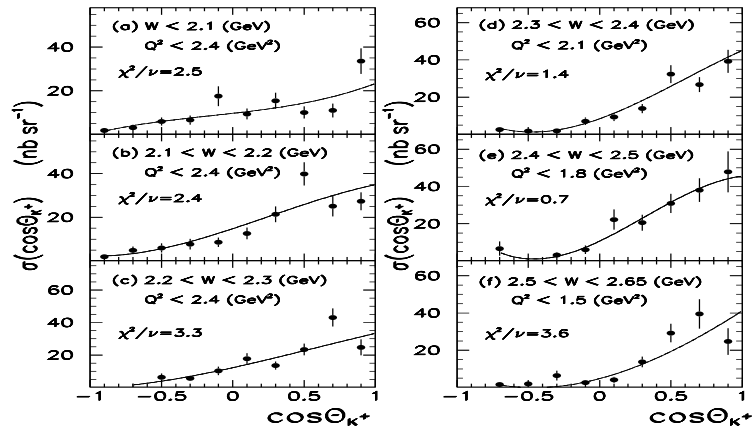


Figure 2: The  $\Lambda(1520)$   $\cos\Theta_{K^+}$  differential cross section distributions for six regions of  $W$ . The error bars are statistical uncertainties only. The solid lines are the results of Legendre polynomial fits to the data. The lower limit  $Q^2 = 0.9 \text{ GeV}^2$  is used for all six distributions.

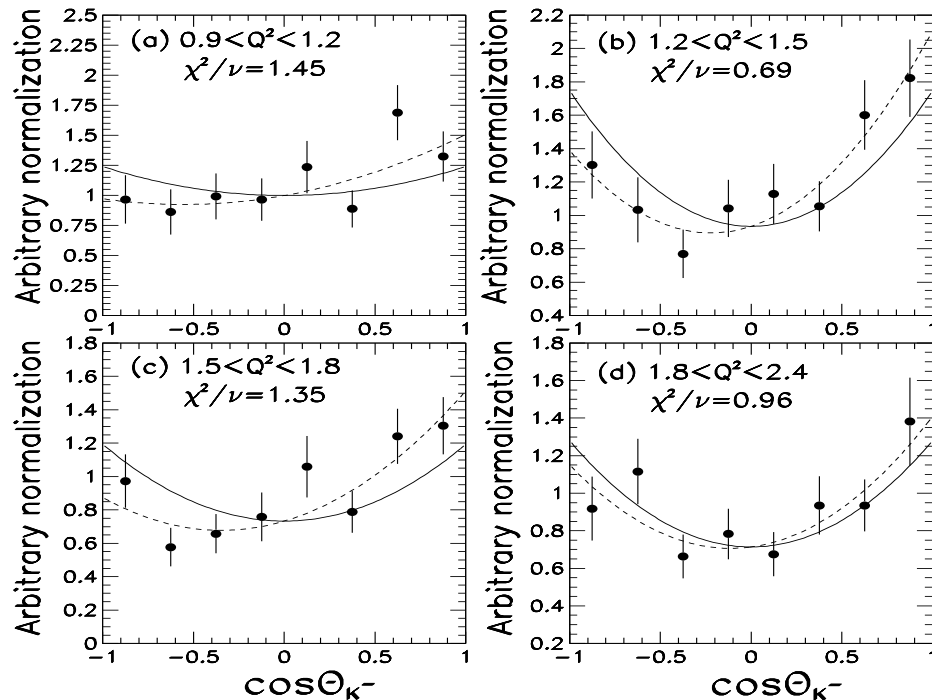


Figure 3: The  $\Lambda(1520) \cos\Theta_{K^-}$  decay angular distribution for four regions of  $Q^2$ . These distributions are averaged over the region of  $W$  from threshold to 2.43 GeV. The error bars are statistical uncertainties only. The solid line in each plot is the fitted contribution from the two spin projection terms of the  $\Lambda(1520)$ , and the dashed line is a fit that also includes a parameterization of the interference between the  $\Lambda(1520)$  and other hyperons.

competition between vector and pseudoscalar meson exchange, and will not be addressed in this report. However, with CLAS it is possible to determine if  $\Lambda(1520)$  electroproduction also proceeds mainly by  $t$ -channel vector meson exchange. This measurement complements the existing photoproduction one, and should greatly facilitate a theoretical understanding of  $\Lambda(1520)$  production. The CLAS electroproduction center-of-mass angular distributions shown in Fig. 2 are consistent with  $t$ -channel dominance.

The  $\Lambda(1520)$  is a  $J^\pi = \frac{3}{2}^-$  baryon, and its  $p - K^-$  decay is a parity conserving strong decay mode. For an  $m_z = \pm\frac{3}{2}$  projection the decay is characterized by a  $\sin^2\Theta_{K^-}$  distribution, while an  $m_z = \pm\frac{1}{2}$  projection has a  $\frac{1}{3} + \cos^2\Theta_{K^-}$  distribution, where  $\Theta_{K^-}$  is the polar angle of the outgoing  $K^-$  decay fragment relative to the incident target proton. The  $t$ -channel helicity frame  $\cos\Theta_{K^-}$  decay angular distributions for four regions of  $Q^2$  are shown in Fig. 3. The photoproduction angular distribution [2] possesses a greatly enhanced  $m_z = \pm\frac{3}{2}$  parentage relative to the electroproduction results presented here. All four of the distributions shown in Fig. 3 demonstrate a large  $\frac{1}{3} + \cos^2\Theta_{K^-}$  contribution, which indicates the electroproduced  $\Lambda(1520)$  hyperons are primarily populating the  $m_z = \pm\frac{1}{2}$  spin projection.

If  $\Lambda(1520)$  electroproduction proceeds exclusively through  $t$ -channel exchange of a spinless kaon, the  $\Lambda(1520)$  spin projection is always  $m_z = \pm\frac{1}{2}$ , and the ratio of the  $m_z = \pm\frac{3}{2}$  to  $m_z = \pm\frac{1}{2}$  populations is zero. On the other hand, if the reaction proceeds exclusively through the transverse exchange of a  $J=1$   $K^*$  vector meson, the ratio of the  $m_z = \pm\frac{3}{2}$  to  $m_z = \pm\frac{1}{2}$  spin projections, if solely

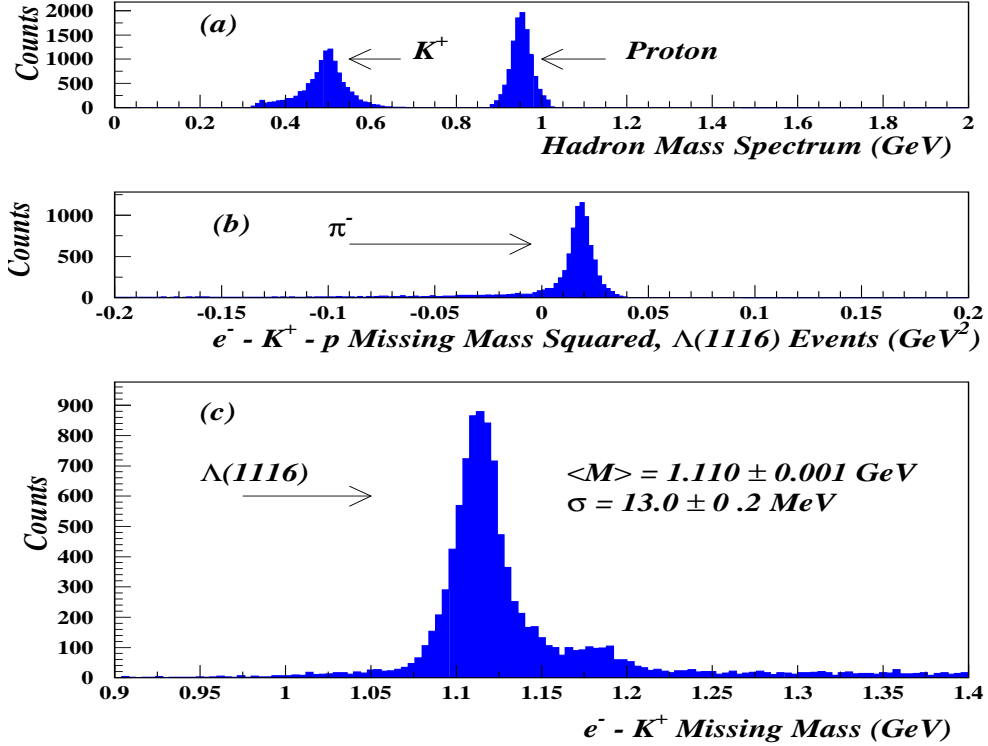


Figure 4: (a) The hadron mass spectrum for events that contain a proton track and a  $K^+$  candidate, for  $\Lambda(1116)$  events. (b) The  $\pi^-$  missing mass spectrum for events in which the  $e^- - K^+$  missing mass is consistent with the  $\Lambda(1116)$  mass. (c) The hyperon mass spectrum for the  $e^- - K^+ - \pi^- - p$  final state.

determined by Clebsch-Gordon coefficients, is 3 to 1. Therefore the electroproduction distributions shown in Fig. 3, and summarized in Table 2, could be evidence for a roughly equal mixture of  $K^*(892)$  and  $K(494)$  contributions, which is a significant departure from what was reported in the photoproduction measurement [2]. This analysis has recently been published in Phys. Rev. C [3].

$Q^2$ range ( $\text{GeV}^2$ )	ratio ( $m_z = \pm\frac{3}{2}$ )/( $m_z = \pm\frac{1}{2}$ )
0.9-1.2	$.806 \pm .125$
1.2-1.5	$.534 \pm .148$
1.5-1.8	$.614 \pm .108$
1.8-2.4	$.558 \pm .108$

Table 2. The ratios of the  $\Lambda(1520)$  electroproduction spin projection parentages for the four regions of  $Q^2$  presented in Fig. 3. A complete discussion of these results is presented in Ref. [3]

### 3 $\Lambda(1116)$ distributions, unpolarized electron beam

In contrast to the  $\Lambda(1520)$ , the  $\Lambda(1116)$  is a  $J^\pi = \frac{1}{2}^+$  baryon. The  $\Lambda(1116)$  decays weakly, and it is therefore possible to deduce the polarization of the  $\Lambda(1116)$  by studying the asymmetry in its decay angular distribution. This provides a unique opportunity to study induced baryon polarization in

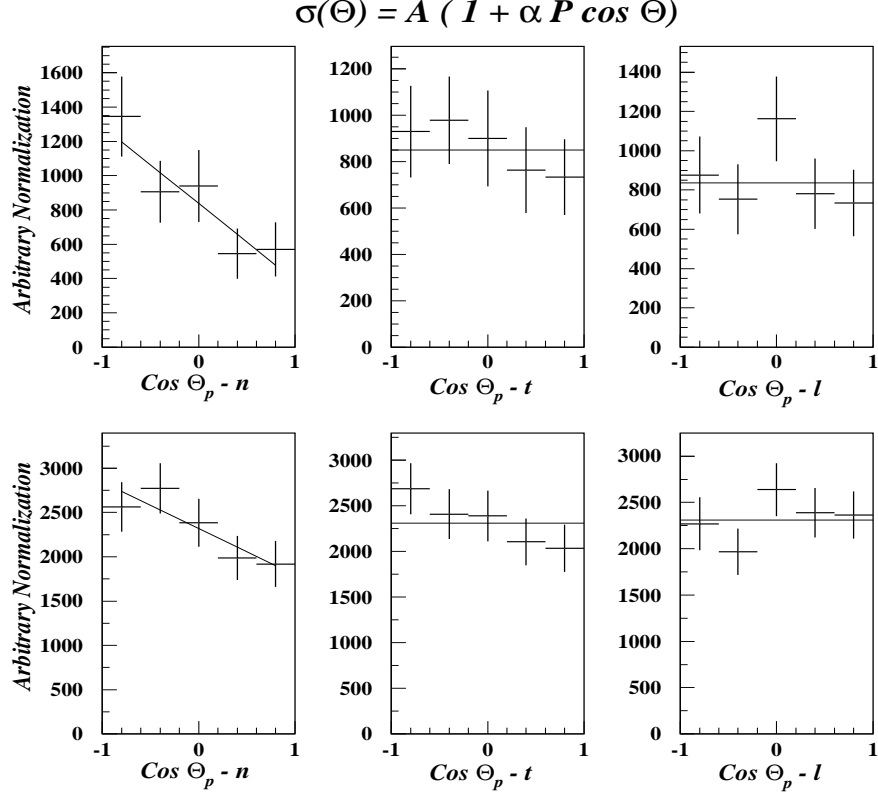


Figure 5: Two examples of  $\Lambda(1116)$  decay angular distributions for three orthogonal projections. The upper trio is for  $1.8 < W < 2.0$  GeV and  $0.0 < \text{Cos}\Theta_p < 0.5$ , while the lower trio is for the same range of  $W$  but  $0.5 < \text{Cos}\Theta_p < 1.0$ . For an unpolarized incident electron beam, only the “ $n$ ” projection, which is normal to the hyperon production plane, is allowed to have a slope to its distribution. The “ $t$ ” and “ $l$ ” projections are in the center-of-mass production plane, and should be flat.

hyperon production. Due to parity constraints on the strong interaction, such polarization is only permitted in the direction normal to the  $\Lambda(1116)$  center-of-mass production plane. The decay angular distribution in the rest frame of the  $\Lambda(1116)$  is of the form  $\sigma(\text{Cos}\Theta_p) = A(1 + \alpha P \text{Cos}\Theta_p)$ , where  $\Theta_p$  is the polar angle of the outgoing proton. The polarization of the  $\Lambda(1116)$  is deduced from the slope of the  $\text{Cos}\Theta_p$  dependence. The relevant hadron spectra are shown in Fig. 4, and two examples of the acceptance corrected yields that are used to derive the  $\Lambda(1116)$  polarization are shown in Fig. 5.

The induced polarization as a function of the center-of-mass quantity  $\text{cos}\Theta_{K^+}$  for two regions of  $W$  are shown in Fig. 6 [4]. Also shown are the results of a photoproduction measurement done at SAPHIR [5] of  $\Lambda(1116)$  induced polarization over the same region of  $W$  studied with CLAS. The photo- and electroproduction measurements both indicate that for low  $W$ , close to threshold, the induced polarization of the  $\Lambda(1116)$  is fairly small, while at higher  $W$  the  $\Lambda(1116)$  polarization is larger and negative, especially for  $\text{Cos}\Theta_{K^+} > 0.0$ . The photo- and electroproduction data also suggest there might be no significant  $Q^2$  dependence to the induced  $\Lambda(1116)$  polarization. One obvious implication of this result is that the  $\Lambda(1116)$  polarization is not very sensitive to the L-T decomposition of the (real or virtual) photon. Once this analysis is complete, it will be interesting to compare the  $W$  dependence of the  $\Lambda(1116)$  induced polarization presented here with the polarization obtained with a nonlepton beam such as a pion or kaon beam.

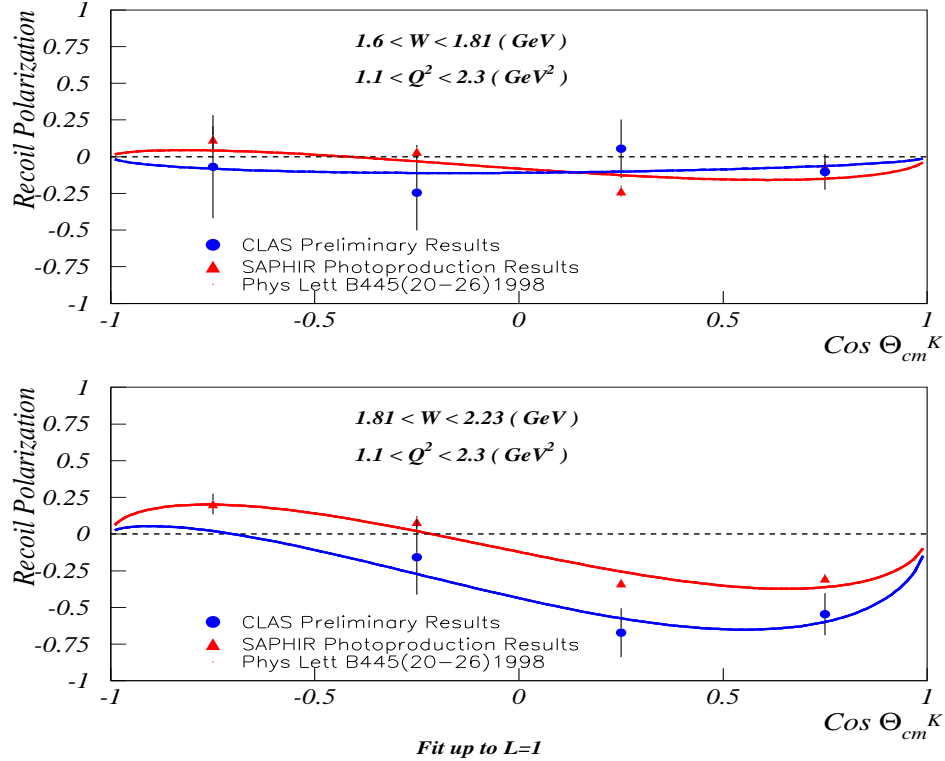


Figure 6: Preliminary CLAS results for the induced  $\Lambda(1116)$  polarization from an unpolarized incident electron beam for two regions of  $W$ , and for  $1.1 < Q^2 < 2.3 \text{ GeV}^2$ . Also shown in these plots are the results of a photoproduction measurement [5].

## 4 Conclusions

The detailed studies of the decay angular distributions of electroproduced hyperons presented here represent a significant addition to existing measurements of hyperon production. These measurements also provide excellent illustrations of the capabilities of the CLAS detector. Nonetheless, these results represent a small fraction of the total studies of hyperon production currently underway on data taken at CLAS. Combined with the other approved analysis activities summarized in Table 1, a much clearer understanding of the strange baryon production processes is emerging.

**Acknowledgments:** The CLAS collaboration is supported by the U.S. Department of Energy and the National Science Foundation, the French Commissariat à l’Energie Atomique, the Italian Istituto Nazionale di Fisica Nucleare, and the Korea Science and Engineering Foundation.

## References

- [1] D. Groom *et al.*, The European Physical Journal C **15**, 1 (2000).
- [2] D. Barber *et al.*, Z. Physik C **7**, 17 (1980).
- [3] S.P. Barrow *et al.*, Phys. Rev. C **64**, 044601 (2001), hep-ex/0105029.
- [4] Data analysis results from S. McAleer (2001).
- [5] M. Q. Tran *et al.*, Phys. Lett. B **445**, 20 (1998).